Magnetic Dendritic Materials for Highly Efficient Adsorption of Dyes and Drugs

Li Zhou,[†,‡] Chao Gao,*[,†] and Weijian Xu*[,‡]

MOE Key Laboratory of Macromolecular Synthesis and Functionalization, Department of Polymer Science and Engineering, Zhejiang University, 38 Zheda Road, Hangzhou 310027, P. R. China, and Institute of Polymer Science and Engineering, College of Chemistry and Chemical Engineering, Hunan University, Changsha 410082, P. R. China

ABSTRACT A versatile and robust adsorbent with both magnetic property and very high adsorption capacity is presented on the basis of functionalization of iron oxide-silica magnetic particles with carboxylic hyperbranched polyglycerol (Fe_3O_4/SiO_2/HPG-COOH). The structure of the resulting product was confirmed by Fourier transform infrared (FTIR) spectra, thermo gravimetric analysis (TGA), zeta-potential, and transmission electron microscopy (TEM). According to the TGA results, the density of the carboxylic groups on the surface of Fe_3O_4/SiO_2/HPG-COOH is calculated to be as high as 3.0 mmol/g, posing a powerful base for adsorbing dyes and drugs. Five kinds of dyes and one representative anticancer drug were chosen to investigate the adsorption capacity of the as-prepared magnetic adsorbent. The adsorbent shows highly efficient adsorption performance for all of the adsorbates especially for the cationic dyes and drug. For example, the saturated adsorption capacity of the Fe_3O_4/SiO_2/HPG-COOH for methyl violet (MV) can reach 0.60 mmol/g, which is much higher than the previous magnetic adsorbents (usually lower than 0.30 mmol/g). 95% of MV and 90% of R6G could be adsorbed within 5 min, and both of the adsorptions reached equilibrium in about 15 min. The adsorption kinetics and isotherm of the adsorbents were investigated in detail and found that the kinetic and equilibrium adsorptions are well-modeled using pseudo-second-order kinetics and Langmuir isotherm model, respectively. In addition, the influences of pH and ionic strength on the adsorption capacity were also examined and found that pH has much greater effect on the adsorption capacity compared with the ionic strength. Regeneration experiments showed that the Fe_3O_4/SiO_2/HPG-COOH can be well-regenerated in ethanol and partially regenerated in 1 M HCl aqueous solution. After regeneration, the magnetic adsorbents can still show high adsorption capacity even for 10 cycles of desorption−adsorption. No obvious decreases of magnetic intensity and aggregation of adsorbents can be observed even after 10 cycles of adsorption−desorption.

KEYWORDS: adsorption • dye • iron oxide • magnetic adsorbent • hyperbranched polymer • Langmuir isotherm

INTRODUCTION

Nowadays, environmental problems have become a global concern because of their impact on public health. The World Health Organization (WHO) estimates that about 25% of the diseases facing humans today occur because long-term exposure to environmental pollution, including air, soil, and water pollution. Improper management of industrial water is one of the main causes of environmental pollution and degradation in many countries. The World Bank (WB) estimates that 17−20% of industrial water pollution comes from textile coloration and treatment.

Actually, dyes are widely used in many industrial fields such as textiles, plastics, paper, coatings, and rubber. It has been estimated that 10−15% of the dyes was lost during the dyeing process and released as effluent (1). The discharge of dyes into water has received global concern because of their overall environmental hazards. The dyes in water are generally difficult to decolorize because of their complex structure and poor biodegradability. The presence of dyes in effluents is highly visible and undesirable even at very low concentration. Some of the dyes are considered toxic and even carcinogenic for human and animal apparatus (2). Therefore, the development of technologies to prevent further dyes discharge and contamination are of great importance. The removal of dyes from aqueous environment has been widely studied and numerous methods such as coagulation (3), membrane filtration (4), adsorption (5), photocatalysis (6), advance oxidation (7), etc., have been developed. Among these methods, the adsorption technique is especially attractive because of its high efficiency, simplicity of design, and ease of operation (8).

Various adsorbents including activated carbons (9), zeolites (10), clays (11), polymeric materials (12), etc., have been used to removal of dyes from wastewater. However, these adsorbents showed either low adsorption capacities or separation inconvenience. Hence, the adsorbent with both characters of high adsorption capacity and facile separation is extremely expected in both science and technology societies. Recently, a unique magnetic carrier technology (MCT) based on the magnetic materials has been reported by several groups (13–17). The attractive property of MCT is that the adsorbents can be facilely separated from sample solution by the application of an external magnetic field. Haik group and Afkhami group reported the adsorption of acridine orange and congo red by γ-Fe_2O_3 magnetic

* To whom correspondence should be addressed. E-mail: chaogao@zju.edu.cn (C.G.); weijxu@hnu.cn (W.X.).

Received for review February 7, 2010 and accepted May 5, 2010

† Zhejiang University.

‡ Hunan University.

DOI: 10.1021/am100114f

nanoparticles, respectively (15, 16). Zhu et al. used chitosan entrapped γ-Fe_2O_3 nanoparticles to adsorb methyl orange (17). Zhang and co-workers first prepared magnetic cellulose beads and then used them to adsorb organic dyes (18). Gong et al. used magnetic multiwalled carbon nanotubes as adsorbents for removal of cationic dyes from aqueous solution (19). Donia and co-workers reported the use of magnetic silica for adsorption of acid orange 10 dyes and found that the adsorption capacity of silica-containing magnetite was higher than the neat magnetite-free silica (20). Bee and co-workers investigated the application of magnetic alginate beads for removal of methylene blue and methyl orange (21, 22). Although these magnetic adsorbents can be facilely recycled from the solution by a magnet, the adsorption capacities are relatively low (lower than 0.1 mmol/g) because of the absence or scarcity of chemically functional groups on the surface of adsorbents. Chen and co-workers reported the use of poly(acrylic acid)- and carboxymethylated chitosan-conjugated Fe_3O_4 magnetic adsorbents for adsorption of basic dyes and acid dyes, respectively (23, 24). Both of the two adsorbents showed relatively high adsorption capacities (about 0.25 mmol/g) for the corresponding dyes, indicating that it would be an effective solution to improve the adsorption capacity by functionalization of magnetic particles with polymer that possesses desired functional groups.

On the basis of previous studies, hyperbranched polymer (HP)-modified magnetic materials should be a more attractive adsorbent compared with the previous magnetic adsorbents because of the advantages of the HP: (1) HP is abundant in functional groups (25–27), which can be used to improve the performance of adsorbents; (2) compared with linear polymer, HP has less or no molecular chain entanglement that may decrease the utilization of functional groups (27, 28); (3) HP can be facilely and cost-effectively synthesized by a one-step method compared with dendrimers (29, 30) that have been widely used as adsorbents for metal ions, proteins and drugs (31–33). Surprisingly, to the best of our acknowledge, no reports on the adsorption of dyes by the HP-functionalized magnetic adsorbents can be found. In addition, for biomedical applications such as protein separation and purification, biosensor and drug carrier, and so forth, magnetic adsorbents with high adsorption capacity are also considerably attractive (34). However, up to now, few reports have been published on the general polymer-functionalized magnetic materials for possible adsorption of both dyes and drugs.

In this paper, we explored a novel magnetic adsorbent based on the carboxylic hyperbranched polyglycerol (HPG)-functionalized iron oxide-silica (Fe_3O_4/SiO_2) hybrids (Fe_3O_4/SiO_2/HPG-COOH). The advantages of this magnetic adsorbent are as follows: (1) the magnetic core can provide a convenient platform for the facile separation; (2) the silica shell can efficiently prevent the aggregation and chemical decomposition of Fe_3O_4 in a harsh environment (35); (3) HPG is biocompatible and thus can be used to adsorb drugs without additional toxicity for the further applications (36–38); (4) HPG possesses favorable structure and numerous functional groups that can be used to improve adsorption capacity compared with linear polymer (36–38); (5) HPG can be grafted from the surface of Fe_3O_4/SiO_2 by only a one-step reaction, and thus the adsorbents can be scalably and cost-effectively produced. It is expected that the Fe_3O_4/SiO_2/HPG-COOH adsorbents would show good adsorption performance: facile magnetic separation and high adsorption capacity. In addition, considering the practical applications, the regeneration of the magnetic adsorbents was also investigated in detail. To the best of our knowledge, this is the first time to report the use of HP-grafted magnetic particles as adsorbents for both dyes and drugs.

EXPERIMENTAL SECTION

Materials. Rhodamine 6G (R6G), rhodamine B (RB), congo red (CR), methyl blue (MB), methyl violet (MV), doxorubicin hydrochloride (DH), tetraethyl orthosilicate (TEOS), iron(III) chloride, iron(II) chloride tetrahydrate, ammonia solution (25 wt %), potassium methylate solution in methanol (CH_3OK, 25 wt %) and glycidol (96%) were purchased from Sigma-Aldrich and used as received. Dioxane, methanol and tetrahydrofuran (THF) were freshly distilled in the presence of calcium hydride before each polymerization. All other reagents were used as received without further purification.

Characterization. Thermogravimetric analysis (TGA) was carried on a Perkin-Elmer (PE) TGA-7 instrument with a heating rate of 20 °C min^{-1} in a nitrogen flow (20 mL min^{-1}). Fourier transform infrared (FTIR) spectra were recorded using a PE Paragon 1000 spectrometer (KBr disk). Zeta potentials were measured at 25 °C using a Zetasizer Nano-Zs (Malvern Instruments, UK). Absorption spectra were recorded at room temperature on a Varian Cary 300 Bio UV—vis spectrophotometer. Transmission electron microscopy (TEM) studies were performed on a JEOL JEL2010 electron microscope at 200 kV. Fluorescence images were obtained with Zeiss LSM-510 confocal laser-scanning microscope using a 1 mW He—Ne laser at 543 nm.

Synthesis. The synthesis of hyperbranched polyglycerol-functionalized Fe_3O_4/SiO_2 particles (Fe_3O_4/SiO_2/HPG) was conducted according to the literature (39, 40). Typically, 150 mg of Fe_3O_4/SiO_2 particles were mixed with 42 μL (1.41 mmol) of potassium methylate (CH_3OK) solution in methanol (25 wt %) and 5 mL of anhydrous tetrahydrofuran (THF) in a flask. The mixture was stirred for 1 h, before which excess methanol was removed by vacuum. Then, 20 mL of anhydrous dioxane was added and the flask was kept in an oil bath at 98 °C. Glycidol (3.0 g, 40.6 mmol) was added dropwise over a period of 15 h. After completion of monomer addition the mixture was stirred for an additional 1 h. The mixture was quenched and dispersed in methanol, and subsequently separated by a magnet and washed with methanol. After repeated washing and separation steps, the resulting Fe_3O_4/SiO_2/HPG solid was dried overnight in a vacuum.

To prepare Fe_3O_4/SiO_2/HPG-COOH hybrids, typically, 100 mg of Fe_3O_4/SiO_2/HPG, 100 mg of triethylamine and 80 mg of succinic anhydride were dispersed in 10 mL of N, N-dimethylformamide (DMF) in a flask. The mixture was stirred at 60 °C for 4.5 h before the resulting solids were separated by a magnet and washed with methanol. After repeated washing and separation steps, the sample was dried overnight in a vacuum, and 156 mg of Fe_3O_4/SiO_2/HPG-COOH was obtained.

Adsorption of Organic Dye and Drug. Six kinds of adsorbates were used in adsorption experiments (see Scheme 1A). Typically, 30 mg of Fe_3O_4/SiO_2/HPG-COOH adsorbent was mixed with 20 mL of solution at the desired dyes concentra-

Scheme 1. (A) Chemical Structures of Dyes and Drug Used for Adsorption; (B) Schematic Illustration of the Structure of Fe_3O_4/SiO_2/HPG-COOH Magnetic Hybrid

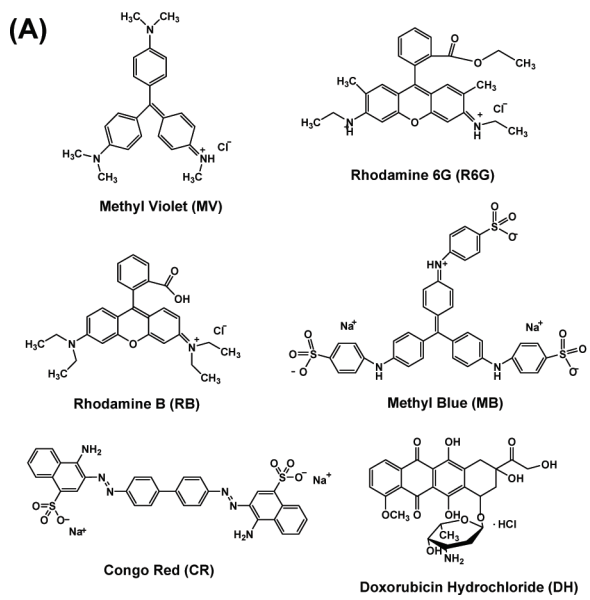

tions, pHs, and ionic strengths at 25 °C. After the agitation at a rate of 100 rpm for 30 min, the solution was centrifuged and small amounts of the liquid were taken to be analyzed by UV−vis absorption spectroscopy by monitoring the absorbance changes at a wavelength of maximum absorbance after being diluted two times. The effect of pH on the amount of dyes removal was analyzed in the pH range from 3 to 10. The solution pH was adjusted by the using of acetic buffer and phosphate buffer. The ionic strength of the organic dyes solution was adjusted by the addition of NaCl (0.1−2.0 M).

Adsorbent Regeneration. For the dye desorption, typically 30 mg of R6G-adsorbed Fe_3O_4/SiO_2/HPG-COOH adsorbent was added into 20 mL of organic solvents or 1 M HCl aqueous solution and the suspensions were then stirred for 30 min. Finally, the adsorbents were collected by a magnet and reused for adsorption again. The supernatant solutions were analyzed by UV−vis spectra. The cycles of desorption−adsorption processes were successively conducted at least 10 times. The used organic solvents are acetone, ether, ethanol, and THF.

RESULTS AND DISCUSSION

Synthesis and Characterization of Fe_3O_4/SiO_2/HPG-COOH Magnetic Adsorbent. To design a functional adsorbent with facile separation and high adsorption capacity properties, grafting carboxylic HPG polymer from the surface of magnetic Fe_3O_4/SiO_2 particles was conducted. The structure of Fe_3O_4/SiO_2/HPG-COOH magnetic adsorbent is schematically illustrated in Scheme 1B. The Fe_3O_4/SiO_2 core−shell particles were synthesized through sol−gel reaction according to the literatures (35, 41). Subsequently, hyperbranched polyglycerol (HPG) was grafted from the surface of Fe_3O_4/SiO_2 by an in situ ring-opening polymerization (37–40). Finally, the hydroxyl groups were transformed into carboxyl groups by reaction with succinic anhydride. All the above reactions were carried out at mild condition, making the large-scale synthesis of magnetic adsorbent with low-cost possible. The facile production is necessary for practical industrial and biological applications.

The whole synthetic process was confirmed by transmission electron microscopy (TEM), Fourier transform infrared (FTIR) spectra, and thermogravimetric analysis (TGA) (Figure S1 and S2). The detailed characterization descriptions of the Fe_3O_4/SiO_2/HPG-COOH magnetic hybrids can be found in the literature (41). According to the TGA results, −COOH density of Fe_3O_4/SiO_2/HPG-COOH is calculated to be ca. 3.0 mmol/g. Such a high content of carboxyl group promises the high adsorption capacity. To further confirm the functionalization of Fe_3O_4/SiO_2, were plotted the influence of pH on the zeta potential of Fe_3O_4/SiO_2 and Fe_3O_4/SiO_2/HPG-COOH in Figure 1. After grafting carboxylic HPG, the zeta-potential decreased significantly over pH 2−10, apparently as a result of ionization of the carboxylic acid. The isoelectric point (iep) of Fe_3O_4/SiO_2/HPG-COOH is found to occur at pH 2.1, which is much lower than the iep value of pH 3.1 for Fe_3O_4/SiO_2. The low iep indicates that the Fe_3O_4/SiO_2/HPG-COOH is negatively charged at the environment of pH 2−10, which will benefit the sorption of positively charged adsorbates. All these characterizations well demonstrate that a dense layer of carboxylic HPG has been successfully grafted from the surface of Fe_3O_4/SiO_2.

Adsorption Properties of the Fe_3O_4/SiO_2/HPG-COOH Magnetic Adsorbent. The aim of preparing $Fe_3O_4/$

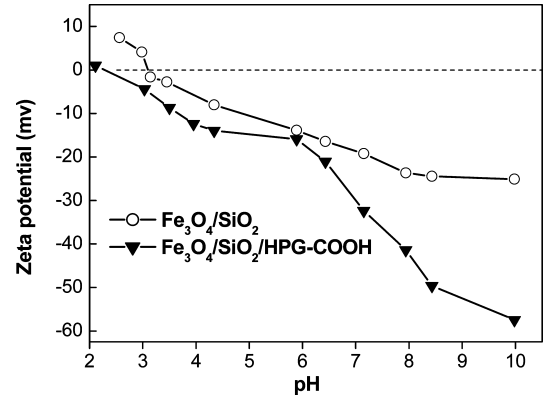

FIGURE 1. Zeta-potentials of Fe_3O_4/SiO_2 and Fe_3O_4/SiO_2/HPG-COOH as a Function of pH.

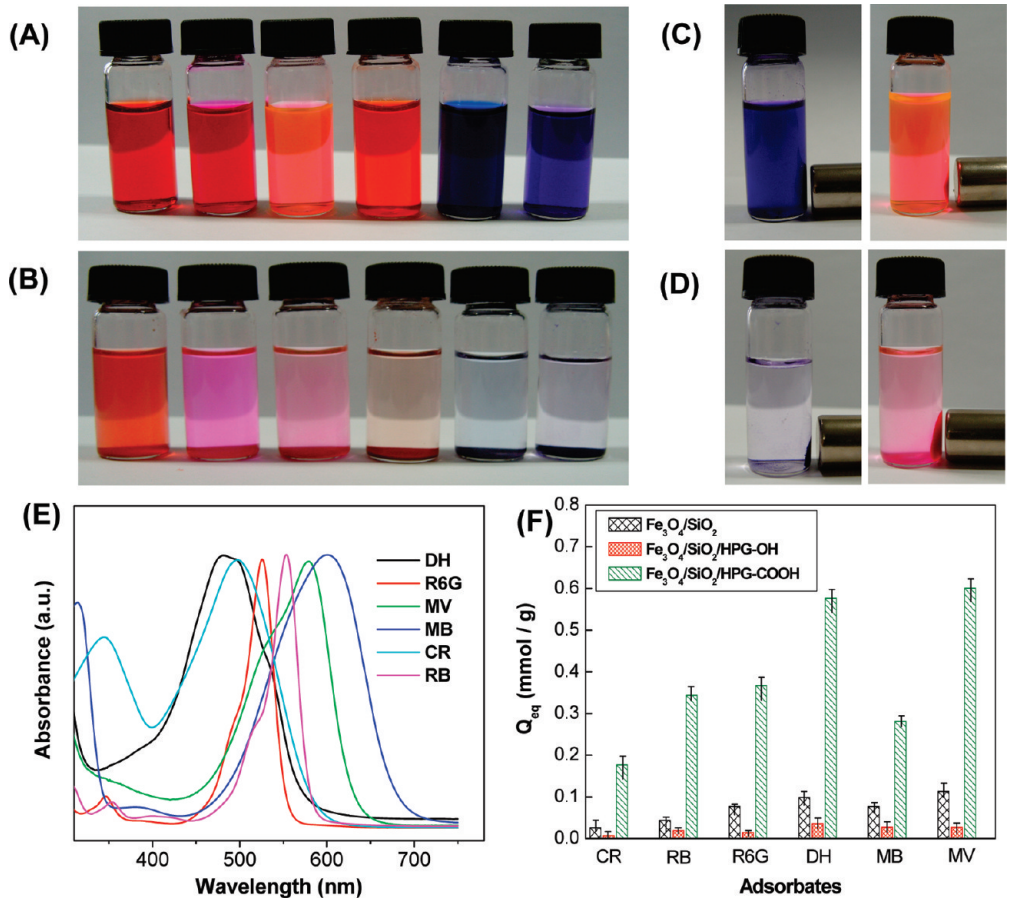

FIGURE 2. Photographs of aqueous solutions of dyes and drugs (A) before and (B) after adsorption on Fe_3O_4/SiO_2/HPG-COOH adsorbent (from left to right: CR, RB, R6G, DH, MB, and MV. Photographs of magnetic separation of MV (left) and R6G (right) after adsorption on (C) Fe_3O_4/SiO_2 and (D) Fe_3O_4/SiO_2/HPG-COOH. (E) Absorption spectra of the dyes and DH drug. (F) Saturated adsorption capacities of Fe_3O_4/SiO_2, Fe_3O_4/SiO_2/HPG, and Fe_3O_4/SiO_2/HPG-COOH for dyes and DH drug.

SiO_2/HPG-COOH is to obtain a novel adsorbent with excellent adsorption capacity and convenient magnetic separation property. Various dyes such as rhodamine B (RB), rhodamine 6G (R6G), methyl violet (MV), methyl blue (MB) and congo red (CR), as well as one of representative anticancer drug, doxorubicin hydrochloride (DH), was chosen to study the adsorption properties of Fe_3O_4/SiO_2/HPG-COOH (the molecular structures of six adsorbates are illustrated in Scheme 1A). Figure 2A shows the aqueous solution of the dyes and the drug of DH, bright color can be clearly observed. After the addition of Fe_3O_4/SiO_2/HPG-COOH for only 1 min, the color of the solution significantly faded except the sample of congo red (Figure 2B). In addition, after the adsorption process, the adsorbent could be easily separated by a magnet as seen in Figure 2D. In contrast, for Fe_3O_4/SiO_2, very little dye was adsorbed though it could also be facilely separated from the solution (Figure 2C). Figure 2E shows the adsorption spectra of the adsorbates. The adsorption capacities of the magnetic adsorbents were determined by comparing the absorption peaks intensity of the adsorbates solutions before and after the adsorption using UV−vis spectroscopy.

Because the saturated adsorption capacities were generally considered as one of the most critical parameters in practical applications for adsorbents, the definitive saturated adsorption capacities of the adsorbents were studied in this paper, as shown in Figure 2F. The amount of dyes or drugs adsorbed at equilibrium was calculated from the following mass balance equation (42)

$$Q_{eq} = \frac{(C_0 - C_{eq})V}{m} \quad (1)$$

where Q_{eq} (mmol/g) is the amount adsorbed per gram of adsorbent at equilibrium, C_0 is the initial concentration of dyes or drugs in the solution (mmol/L), C_{eq} is the concentration of dyes or drugs at equilibrium (mmol/L), V is the volume of the solution (L), and m is the mass of the adsorbent used (g). For comparison, Fe_3O_4/SiO_2 and Fe_3O_4/SiO_2/HPG were also investigated. As we can see, for almost all of the adsorbates (except CR), Fe_3O_4/SiO_2/HPG-COOH exhibited excellent adsorption capacities. Especially for MV dye and DH drug, the adsorption capacities reached as high as 0.60 and 0.57 mmol/g, respectively, which are much higher than the previous magnetic adsorbents. In contrast, for Fe_3O_4/SiO_2 and Fe_3O_4/SiO_2/HPG, the values of Q_{eq} for the adsorbates were not higher than 0.12 mmol/g. Therefore, we can speculate that the strong adsorption ability of the Fe_3O_4/SiO_2/HPG-COOH is derived from the strong interactions between the surface $-COO^-$ negative groups and positive functional groups of adsorbates such as $-NH_2$, $-NH-$, and $=N^+H-$. Because the CR and MB contain negative $-SO_3^-$ groups,

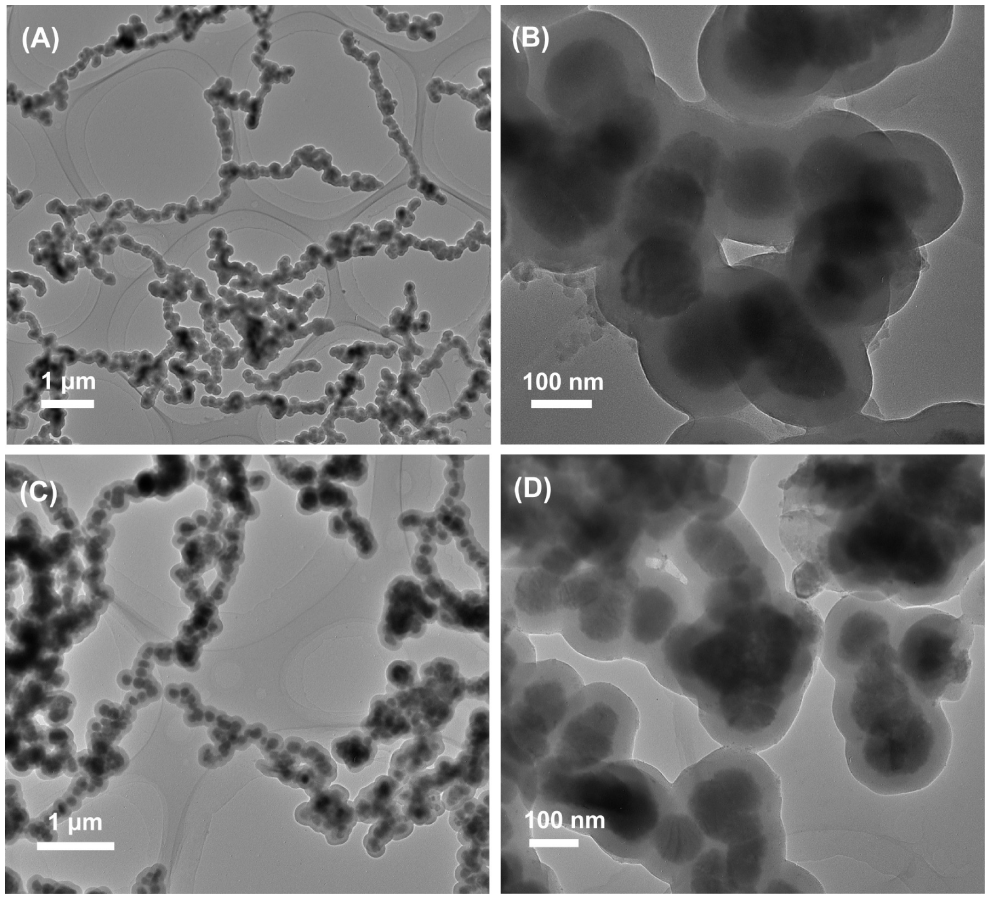

FIGURE 3. TEM images of Fe_3O_4/SiO_2/HPG-COOH (A, B) before and (C, D) after adsorption of R6G at different magnifications.

their interactions with the Fe_3O_4/SiO_2/HPG-COOH are much weaker than others, thus the Q_{eq} for CR and MB are relatively low (Scheme 1A). Thereby, our Fe_3O_4/SiO_2/HPG-COOH magnetic adsorbents are highly suitable for the adsorption of cationic dyes or drugs. Incidentally, it is also believed that if the hydroxyl groups of the HPG are transformed into positive groups such as amino groups the obtained magnetic hybrids would work well for anionic dyes, indicating the high compatibility and versatility of our adsorbent precursor. The relevant work is in progress, and will be reported later. In addition, to probe whether the adsorption of dyes can cause aggregations and degradations of the adsorbents, TEM measurements of the R6G-adsorbed adsorbents were conducted. As shown in Figure 3, no obvious change for the Fe_3O_4/SiO_2/HPG-COOH adsorbents before and after the adsorption of R6G can be detected, suggesting that the magnetic adsorbents are very stable in the application of dye adsorption. To further understand the adsorption process of the Fe_3O_4/SiO_2/HPG-COOH, we selected R6G and MV cationic dyes to investigate the adsorption kinetics and isotherms.

Adsorption Kinetics. The effect of the contact time on the adsorption of MV and R6G dyes by Fe_3O_4/SiO_2/HPG-COOH is presented in Figure 4 and Figure 5A. The initial concentrations of MV and R6G are 0.32 and 0.27 mmol/L, respectively. From an economical point of view, the contact time required to reach equilibrium is an important parameter in the practical applications. As can be seen, almost

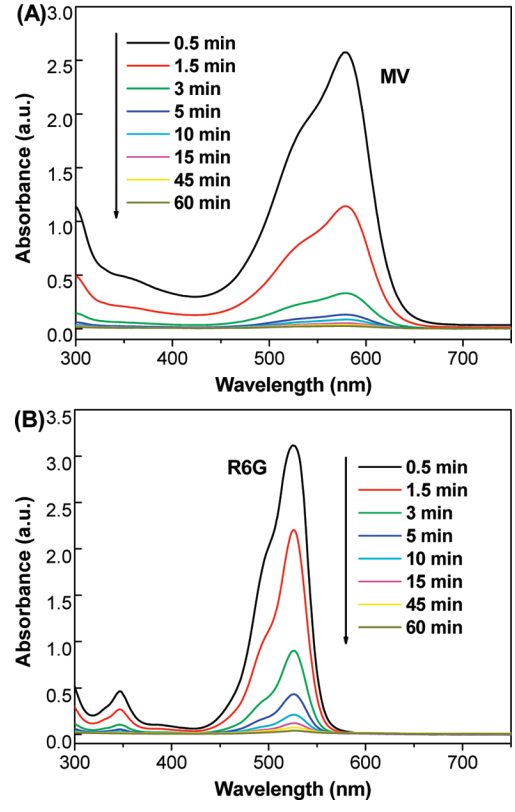

FIGURE 4. Absorption spectra of (A) MV and (B) R6G at different adsorption times.

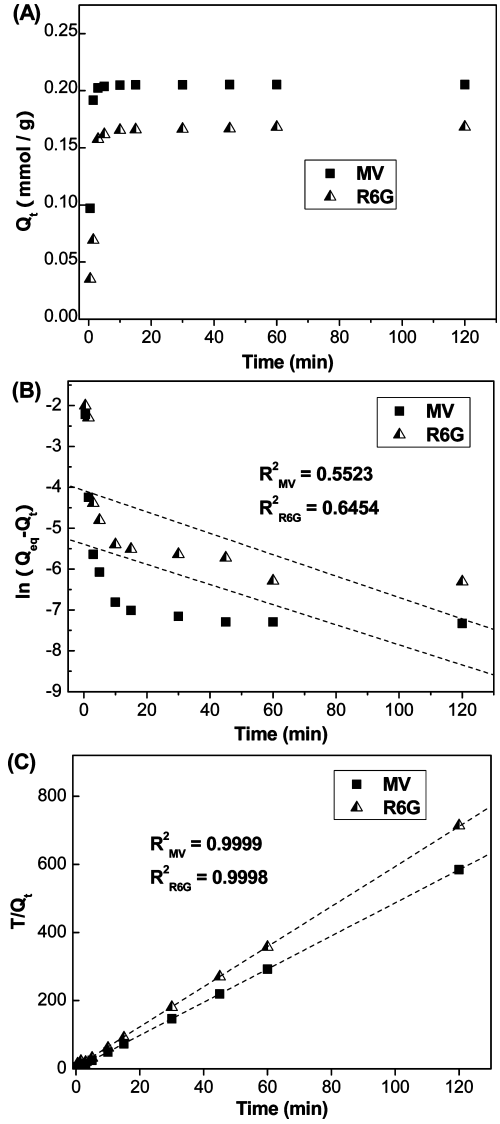

FIGURE 5. (A) Effect of contact time on the adsorption of MV and R6G by Fe_3O_4/SiO_2/HPG-COOH magnetic adsorbent at pH 6.7 and 25 °C. The initial dyes concentrations of MV and R6G are 0.32 mmol/L and 0.27 mmol/L, respectively. Plots of (B) first- and (C) second-order rates for adsorption of MV and R6G onto Fe_3O_4/SiO_2/HPG-COOH adsorbent.

95% of MV and 90% of R6G were adsorbed within 5 min, and both of the adsorptions reached equilibrium in about 15 min.

To well-study the adsorption mechanism and kinetics, two well-known adsorption models, pseudo-first- and pseudo-second-order equations, were used to investigate the adsorption kinetics of the Fe_3O_4/SiO_2/HPG-COOH adsorbent (43, 44). The pseudo-first-order equation is

$$\frac{dQ_t}{dt} = k_1(Q_{eq} - Q_t) \tag{2}$$

where Q_{eq} and Q_t (mmol/g) are the amounts of dye adsorbed at the equilibrium (min) and time t, respectively; k_1 is the pseudo-first-order rate constant (min). After definite integration by applying the initial conditions $Q_t = 0$ at $t = 0$ and $Q_t = Q_t$ at $t = t$, eq 2 becomes:

$$\ln(Q_{eq} - Q_t) = \ln Q_{eq} - k_1 t \tag{3}$$

The plot of $\ln(Q_{eq} - Q_t)$ versus t should give a straight line with slope $-k_1$. In fact, however, the correlation coefficients for MV and R6G are 0.5523 and 0.6454, respectively (Figure 5B). Such low correlation coefficients suggested the poor agreement of pseudo-first-order model with the experimental data.

The pseudo-second-order equation is as described below

$$\frac{dQ_t}{dt} = k_2(Q_{eq} - Q_t)^2 \tag{4}$$

Integrating this equation by applying the initial conditions $Q_t = 0$ at $T = 0$ and $Q_t = Q_t$ at $T = t$, eq 4 becomes

$$\frac{t}{Q_t} = \left(\frac{1}{k_2 Q_{eq}^2}\right) + \frac{t}{Q_{eq}} \tag{5}$$

As shown in Figure 5C, two linear plots of t/Q_t against t give high correlation coefficients of 0.9999 and 0.9998 for MV and R6G, respectively. Therefore, the adsorptions are well-agreed with the pseudosecond-order model.

Adsorption Isotherms. Isotherms studies can describe how the adsorbates interact with adsorbents, which is the most important parameter for designing a desired adsorption system (45). Figure 6A shows the equilibrium isotherms for the adsorptions of R6G and MV. The two famous Freundlich and Langmuir isotherm models have been widely used in adsorption isotherm studies and were also used in this work to fit the experimental data for R6G and MV on Fe_3O_4/SiO_2/HPG-COOH magnetic adsorbents (46).

The linearized form of the Freundlich isotherm can be given as follows

$$\ln Q_{eq} = \ln K_F + b_F \ln C_{eq} \tag{6}$$

where C_{eq} (mmol/L) is the equilibrium concentration of the dyes in the solution, Q_{eq} (mmol/g) is the amount of dye adsorbed at the equilibrium, K_F is the Freundlich constant, and b_F is a constant depicting the adsorption intensity. The value of $\ln Q_{eq}$ against $\ln C_{eq}$ according to the experimental isotherm data is shown in Figure 6B, and the corresponding correlation coefficients for adsorption of R6G and MV are 0.6553 and 0.8459, respectively. The low correlation coefficients indicated the poor agreement of the Freundlich isotherm with our adsorption cases.

According to Langmuir theory, it assumes that the adsorption occurs at a specific homogeneous site within adsorbent, all sites are equivalent, and there are no interactions between adsorbate molecules. The form of the Langmuir isotherm is as follows

$$\frac{C_{eq}}{Q_{eq}} = \frac{C_{eq}}{Q_{max}} + \frac{1}{Q_{max}K_L} \quad (7)$$

where C_{eq} (mmol/L) is the equilibrium concentration of the dyes in the solution, Q_{eq} (mmol/g) is the amount of dye adsorbed at the equilibrium, Q_{max} (mmol/g) is the maximum capacity of the adsorbent, and K_L (L/mmol) is the Langmuir adsorption constant. The plots of C_{eq}/Q_{eq} versus C_{eq} in Figure 6C present straight lines with correlation coefficients for both R6G and MV are 0.9999, indicating that the adsorption of R6G and MV on the Fe_3O_4/SiO_2/HPG-COOH magnetic adsorbents obey the Langmuir adsorption isotherm. In addition, from the slopes 0.2687 and 0.1662 for R6G and MV, respectively, the maximum adsorption capacity of the Fe_3O_4/SiO_2/HPG-COOH is calculated to be 0.37 mmol/g for R6G and 0.60 mmol/g for MV. These values are well in accordance with the saturated adsorption capacities shown in Figure 2F, confirming in turn the fact that the adsorption obeys the Langmuir model.

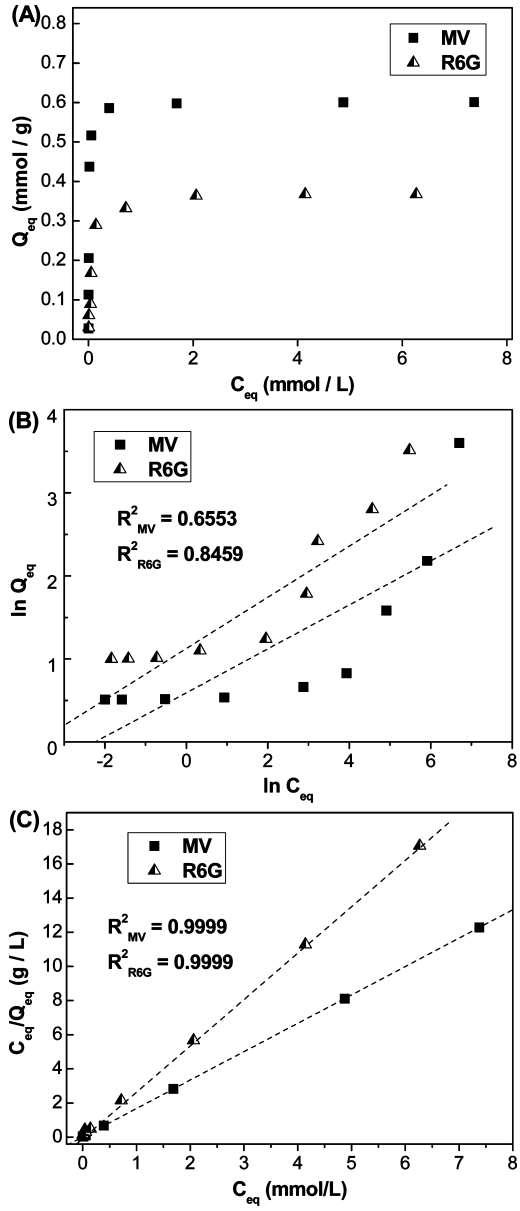

FIGURE 6. (A) Adsorption isotherms for the adsorption of MV and R6G on magnetic Fe_3O_4/SiO_2/HPG-COOH adsorbent at pH 6.7 and 25 °C. (B) The values of ln Q_{eq} against lnC_{eq} based on the Freundlich isotherm model. (C) The linear dependence of C_{eq}/Q_{eq} on C_{eq} based on the Langmuir isotherm model.

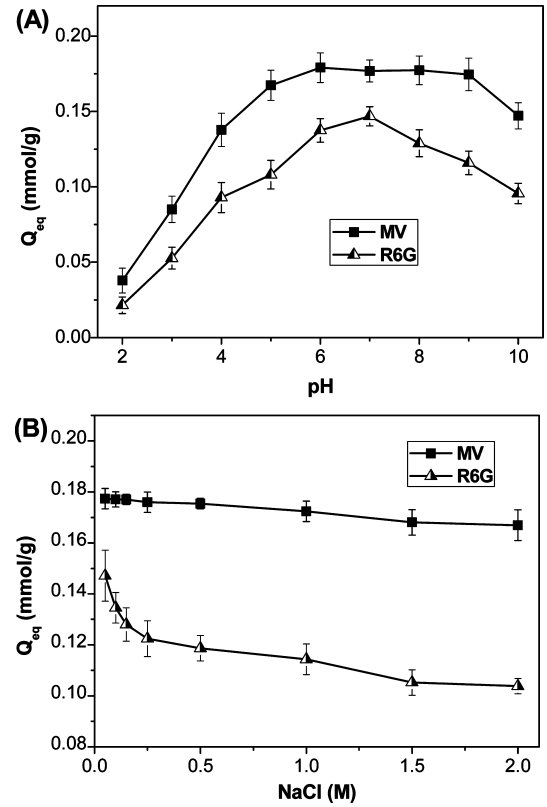

FIGURE 7. (A) Effect of pH on the adsorption of MV and R6G by Fe_3O_4/SiO_2/HPG-COOH adsorbent at 25 °C. (B) Effect of ionic strength on the adsorption of MV and R6G by Fe_3O_4/SiO_2/HPG-COOH at pH 6.7 and 25 °C. In both A and B, the initial dyes concentrations of MV and R6G are 0.28 and 0.24 mmol/L, respectively.

Influence of pH and Ions Strength. The effects of pH and ions strength on the adsorption of dyes by Fe_3O_4/SiO_2/HPG-COOH were studied to gain further insight into the adsorption process. As shown in Figure 7A, no significant influence of pH on dye adsorption for both R6G and MV can be found even the pH in the wide range of 4−10. The excellent adsorption ability can be attributed to the fact that the Fe_3O_4/SiO_2/HPG-COOH has very small positive zeta potential when the pH in the range of 4−10 (Figure 1), and therefore, the electrostatic attraction between the adsorbent and dye are strong. This is very important since the industrial effluents or wastewaters usually have pH values in the relatively acidic range. On the other hand, the adsorption capacity decreases obviously at pH 3. This can possibly be attributed to the increase of competition between protons and the adsorption sites on the surface of Fe_3O_4/SiO_2/HPG-COOH for the dyes. According to this phenomenon, the adsorbed dyes can be released from the adsorbents at a very low pH after the adsorption process, and thereby, the adsorbent can be reused.

The influence of ionic strength on the adsorption is shown in Figure 7B. As the concentration of NaCl increased to 2.0 M, the adsorption capacity for MV was not obviously af-

fected, whereas for R6G, the adsorption capacity decreased by 31%. So the influence of ionic strength is more important for the adsorption of R6G. The different adsorption performance of the Fe_3O_4/SiO_2/HPG-COOH on dyes at the same ionic strength may be ascribed to the different interaction between dyes and electrolytes.

Regeneration Studies. From an application point of view, the regeneration capability of the adsorbent is very important since the dyes can be recycled and the adsorbent can be regenerated for next applications. However, the regeneration of the magnetic adsorbents has rarely been reported, probably because of the bad regeneration performance of the adsorbents. Herein, the desorption experiments were first conducted in the aqueous solution of HCl (1 M) for R6G-adsorbed adsorbent. After the desorption, the regenerated Fe_3O_4/SiO_2/HPG-COOH magnetic adsorbent was reused, and 10 cycles of desorption−adsorption were performed (Figure 8). After 10 cycles of the desorption−adsorption, the magnetic adsorbents did not show obvious decrease of magnetic intensity and the adsorbent can still be collected from the solution within 30 s using a magnet of 4000 Gs (Figure 8A). Meanwhile, fluorescence images of R6G-adsorbed Fe_3O_4/SiO_2/HPG-COOH after 6 cycles of desorption−adsorption showed that no obvious aggregations can be found, suggesting that the adsorbent is stable in an acidic solution (Figure 9). The regeneration results showed that the adsorption capacity decreased not more than 20% after 3 cycles of desorption-adsorption compared with the original adsorption capacity (Figure 8B and 8C). However, as the cycles increased to 10, only 31.7% of the adsorption capacity was retained. This decrease phenomenon is possibly attributed to that the competition between protons and the adsorbed dyes is not strong enough to completely regenerate the adsorbents. In addition, for the dyes adsorbed into the interior cavities of the HPG, hindrance effect may also lead to poor performance of regeneration. As the cycles increase, only part of the external adsorbed dyes can be desorbed. Although the adsorption capacity (0.11 mmol/g) after 10 cycles of the desorption−adsorption is still high compared with other reported adsorbents, it is no doubt that the decrease of the adsorption capacity would seriously limit the practical applications of the magnetic adsorbent. To well regenerate the adsorbents, other organic medium were investigated including acetone, ether, ethanol, and THF. To our delight, the Fe_3O_4/SiO_2/HPG-COOH adsorbents can be well-regenerated in ethanol. As shown in Figure 8B and 8C, more than 86% of adsorption capacity could be retained even after 10 cycles of desorption−adsorption. This good performance of regeneration can be attributed to the sufficiently charge competition in ethanol medium (15). Meanwhile, the dyes can be recycled after evaporation of the ethanol. In addition, it should not be forgotten that the Fe_3O_4/SiO_2/HPG-COOH adsorbent can be facilely recycled by a magnet. Therefore, our magnetic adsorbent can be readily recycled from the industrial water and then reused for several times with high adsorption capacity, promising its great potential in real applications.

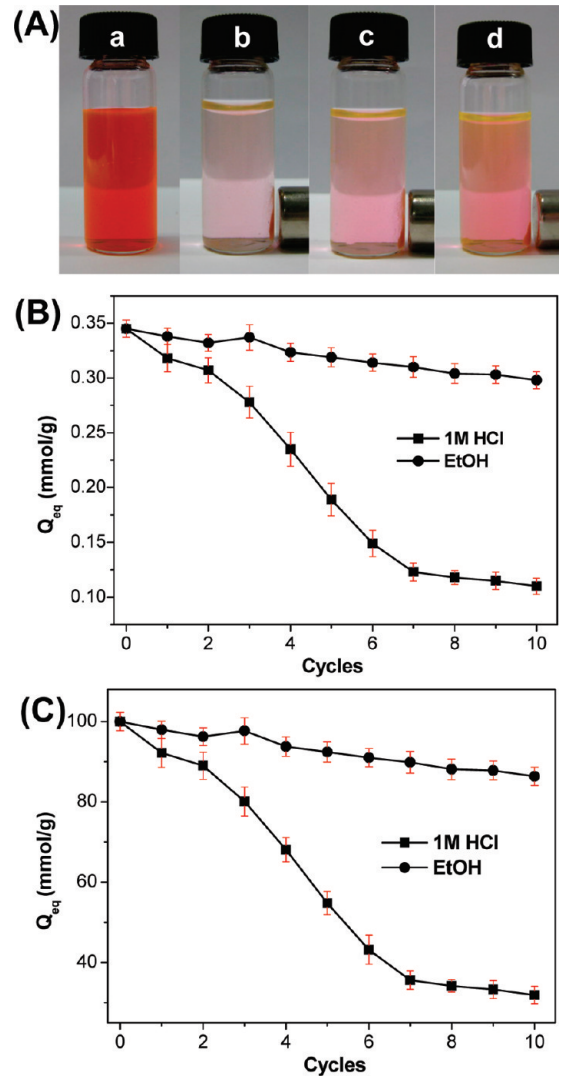

FIGURE 8. (A) Photographs of aqueous solutions of R6G (a) before adsorption and after adsorption by the Fe_3O_4/SiO_2/HPG-COOH adsorbents which have been used for (b) 1, (c) 3, and (d) 5 cycles of desorption-adsorption (desorption in 1 M HCl aqueous solution). (B) Adsorption capacity of Fe_3O_4/SiO_2/HPG-COOH in 10 successive cycles of desorption-adsorption (desorption in 1 M HCl aqueous solution or ethanol). (C) Adsorption ratio of the Fe_3O_4/SiO_2/HPG-COOH in 10 cycles of desorption−adsorption compared with the original adsorption capacity (desorption in 1 M HCl aqueous solution or ethanol).

CONCLUSIONS

We present here a simple approach for production of carboxylic hyperbranched polyglycerol-grafted Fe_3O_4/SiO_2 magnetic adsorbent. This adsorbent combined the both features of Fe_3O_4 and HPG, facile magnetic separation and numerous surface functional groups. The obtained magnetic adsorbent exhibited very high adsorption capacity for cationic dyes and drugs because of the strong electrostatic attraction between its negative surface groups and the adsorbates. The adsorption kinetics and isotherms studies demonstrated that the adsorption process obeyed the pseudo-second-order kinetics and Langmuir isotherm model, respectively. The adsorption capacity can be affected by pH especially at low pH and selectively affected by ionic strength. In addition, the adsorbent can be regenerated in ethanol without serious decrease of its adsorption capacity. Considering the facile fabrication process and

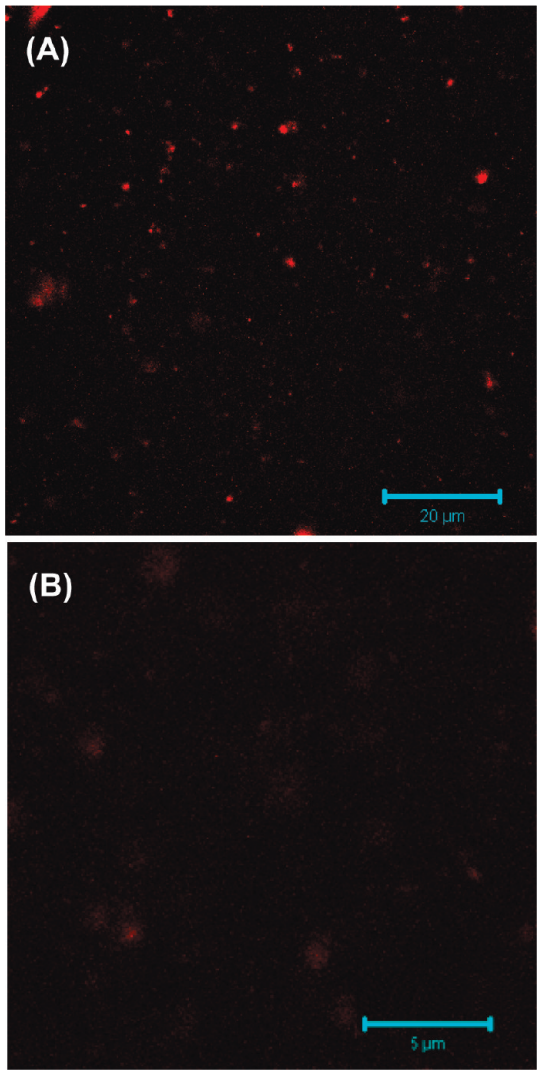

FIGURE 9. Confocal fluorescence images of Fe_3O_4/SiO_2/HPG-COOH after 6 cycles of desorption−adsorption of R6G in 1 M HCl at (A) low and (B) high magnification. Scale bars: (A) 20 and (B) 5 μm.

high adsorption capacity of this magnetic adsorbent, it is firmly believed that this fascinating adsorbent will find great potential applications in the adsorptions of dyes from wastewaters and industrial effluents, and drug delivery.

Acknowledgment. This work was financially supported by the National Natural Science Foundation of China (50773038 and 20974093), National Basic Research Program of China (973 Program) (2007CB936000), Science Foundation of Chinese University, and the Foundation for the Author of National Excellent Doctoral Dissertation of China (200527).

Supporting Information Available: TEM images of Fe_3O_4, Fe_3O_4/SiO_2, and Fe_3O_4/SiO_2/HPG; FT-IR spectra and TGA weight loss curves of Fe_3O_4/SiO_2, Fe_3O_4/SiO_2/HPG, and Fe_3O_4/SiO_2/HPG-COOH (PDF). This material is available free of charge via the Internet at http://pubs.acs.org.

REFERENCES AND NOTES

(1) Al-Ghouti, M. A.; Khraisheh, M.; Allen, S. J.; Ahmad, M. N. *J. Environ. Manage.* **2003**, *69*, 229–238.
(2) Uddin, M. T.; Islam, M. A.; Mahmud, S.; Rukanuzzaman, M. *J. Hazard. Mater.* **2009**, *164*, 53–60.
(3) Shi, B. Y.; Li, G. H.; Wang, D. S.; Feng, C. H.; Tang, H. X. *J. Hazard. Mater.* **2007**, *143*, 567–574.
(4) Lee, J. W.; Choi, S. P.; Thiruvenkatachari, R.; Shim, W. G.; Moon, H. *Water Res.* **2006**, *40*, 435–444.
(5) Mahanta, D.; Madras, G.; Radhakrishnan, S.; Patil, S. *J. Phys. Chem. B* **2008**, *112*, 10153–10157.
(6) Fernández, J.; Kiwi, J.; Lizama, C.; Freer, J.; Baeza, J.; Mansilla, H. D. *J. Photochem. Photobiol., A* **2002**, *151*, 213–219.
(7) Chen, W. X.; Lu, W. Y.; Yao, Y. Y.; Xu, M. H. *Environ. Sci. Technol.* **2007**, *41*, 6240–6245.
(8) Wong, Y. C.; Szeto, Y. S.; Cheung, W. H.; Mckay, G. *Langmuir* **2003**, *19*, 7888–7894.
(9) Al-Degs, Y.; Khraisheh, M. A. M.; Allen, S. J.; Ahmad, M. N. *Water Res.* **2000**, *34*, 927–935.
(10) Lee, C. K.; Liu, S. S.; Juang, L. C.; Wang, C. C.; Lin, K. S.; Lyu, M. D. *J. Hazard. Mater.* **2007**, *147*, 997–1005.
(11) Espantaleón, A. G.; Nieto, J. A.; Fernández, M.; Marsal, A. *Appl. Clay. Sci.* **2003**, *24*, 105–110.
(12) Yu, Y.; Zhuang, Y. Y.; Wang, Z. H.; Qiu, M. Q. *Ind. Eng. Chem. Res.* **2003**, *42*, 6898–6903.
(13) Qu, S.; Huang, F.; Yu, S. N.; Chen, G.; Kong, J. L. *J. Hazard. Mater.* **2008**, *160*, 643–647.
(14) Mak, S. Y.; Chen, D. H. *Dyes Pigm.* **2004**, *61*, 93–98.
(15) Qadri, S.; Ganoe, A.; Haik, Y. *J. Hazard. Mater.* **2009**, *169*, 318–323.
(16) Afkhami, A.; Moosavi, R. *J. Hazard. Mater.* **2010**, *174*, 398–403.
(17) Zhu, H. Y.; Jiang, R.; Xiao, L. *Appl. Clay Sci.* **2010**, *48*, 522–526.
(18) Luo, X. G.; Zhang, L. N. *J. Hazard. Mater.* **2009**, *171*, 340–347.
(19) Gong, J. L.; Wang, B.; Zeng, G. M.; Yang, C. P.; Niu, C. G.; Niu, Q. Y.; Zhou, W. J.; Liang, Y. *J. Hazard. Mater.* **2009**, *164*, 1517–1522.
(20) Atia, A. A.; Donia, A. M.; Al-Amrani, W. A. *Chem. Eng. J.* **2009**, *150*, 55–62.
(21) Rocher, V.; Siaugue, J. M.; Gabuil, V.; Bee, A. *Water Res.* **2008**, *42*, 1290–1298.
(22) Rocher, V.; Bee, A.; Siaugue, J. M.; Gabuil, V. *J. Hazard. Mater.* **2010**, *178*, 434–439.
(23) Liao, M. H.; Chen, D. H. *J. Mater. Chem.* **2002**, *12*, 3654–3659.
(24) Chang, Y. C.; Chen, D. H. *Macromol. Biosci.* **2005**, *5*, 254–261.
(25) Karak, N.; Maiti, S. In *Dendrimers and Hyperbranched Polymers: Synthesis to Applications*; MD Publications: New Delhi, India, 2008.
(26) Fréchet, J. M. J.; Tomalia, D. A. In *Dendrimers and Other Dendritic Polymers*; Wiley−VCH: New York, 2001.
(27) Gao, C.; Yan, D. *Prog. Polym. Sci.* **2004**, *29*, 183–275.
(28) Sunder, A.; Hanselmann, R.; Frey, H.; Mülhaupt, R. *Macromolecules* **1999**, *32*, 4240–4246.
(29) Wang, W. X.; Zheng, Y.; Roberts, E.; Duxbury, C. J.; Ding, L. F.; Irvine, D. J.; Howdle, S. M. *Macromolecules* **2007**, *40*, 7184–719.
(30) Wang, W. X.; Yan, D. Y.; Bratton, D.; Howdle, S. M.; Wang, Q.; Lecomte, P. *Adv. Mater.* **2003**, *15*, 1348–1352.
(31) Diallo, M. S.; Balogh, L.; Shafagati, A.; Johnson, J. H.; Goddard, W. A.; Tomalia, D. A. *Environ. Sci. Technol.* **1999**, *33*, 820–824.
(32) Medina, S. H.; El-Sayed, M. E. H. *Chem. Rev.* **2009**, *109*, 3141–3157.
(33) Su, C. J.; Liu, Y. C.; Chen, H. L.; Li, Y. C.; Lin, H. K.; Liu, W. L.; Hsu, C. S. *Langmuir* **2007**, *23*, 975–978.
(34) Horák, D.; Babič, M.; Macková, H.; Beneš, M. J. *J. Sep. Sci.* **2007**, *30*, 1751–1772.
(35) Shao, D. D.; Xu, K. K.; Song, X. J.; Hu, J. H.; Yang, W. L.; Wang, C. C. *J. Colloid Interface Sci.* **2009**, *336*, 526–532.
(36) Wilms, D.; Stiriba, S. E.; Frey, H. *Acc. Chem. Res.* **2010**, *43*, 129–141.
(37) Zhou, L.; Gao, C.; Xu, W. J. *Macromol. Chem. Phys.* **2009**, *210*, 1011–1018.
(38) Zhou, L.; Gao, C.; Xu, W. J.; Wang, X.; Xu, Y. H. *Biomacromolecules* **2009**, *10*, 1865–1874.
(39) Zhou, L.; Gao, C.; Xu, W. J. *Langmuir* **2010**; DOI:10.1021/la100556p.
(40) Zhou, L.; Gao, C.; Xu, W. J. *ACS Appl. Mater. Interfaces* **2010**, *2*, 1211–1219.
(41) Stöber, W.; Fink, A.; Bohn, E. *J. Colloid Interface Sci.* **1968**, *26*, 62–69.
(42) Crini, G. *Dyes Pigm.* **2008**, *77*, 415–426.
(43) Wasay, S. A.; Haron, M. J.; Uchiumi, A.; Tokunaga, S. *Water Res.* **1999**, *30*, 1143–1148.
(44) Ho, Y. S.; Mckay, G. S. *Water Res.* **2000**, *34*, 735–742.
(45) Hu, Q. H.; Qiao, S. Z.; Haghseresht, F.; Wilson, M. A.; Liu, G. Q. *Ind. Eng. Chem. Res.* **2006**, *45*, 733–738.
(46) Al-Degs, Y. S.; El-Barghouthi, M. I.; El-Sheikh, A. H.; Walker, G. M. *Dyes Pigm.* **2008**, *77*, 16–23.

AM100114F